Engineering Conferences International
ECI Digital Archives

10th International Conference on Circulating Fluidized Beds and Fluidization Technology - CFB-10

Refereed Proceedings

Spring 5-2-2011

Energetic Optimization of the Lignin Pyrolysis for the Production of Aromatic Hydrocarbons

Miika Franck
Institute of Solids Process Engineering and Particle Technology Hamburg University of Technology, Hamburg, Germany

Ernst-Ulrich Hertge
Institute of Solids Process Engineering and Particle Technology Hamburg University of Technology, Hamburg, Germany

Stefan Heinrich
Institute of Solids Process Engineering and Particle Technology Hamburg University of Technology, Hamburg, Germany

Bea Lorenz
Institute of Solids Process Engineering and Particle Technology Hamburg University of Technology, Hamburg, Germany

Joachim Werther
Institute of Solids Process Engineering and Particle Technology Hamburg University of Technology, Hamburg, Germany

ENERGETIC OPTIMIZATION OF THE LIGNIN PYROLYSIS FOR THE PRODUCTION OF AROMATIC HYDROCARBONS

Miika Franck, Ernst-Ulrich Hartge, Stefan Heinrich, Bea Lorenz, Joachim Werther
Institute of Solids Process Engineering and Particle Technology
Hamburg University of Technology, Hamburg, Germany

ABSTRACT

The energy supply of the endothermic lignin pyrolysis process in a circulating fluidized bed is to be achieved by recirculation of bed material, which is heated by combustion of the by-products char and permanent gases in a separate combustor. The feasibility of this concept is examined by the investigation of the yield of the by-products in pyrolysis experiments, char combustion kinetics, the pyrolysis energy demand and the combustion energy of the char and the non-condensable gases. It is shown that the integrated pyrolysis-combustion process is feasible and even produces an energy surplus of 4 MJ/kg raw lignin, which can be used in the downstream processing of pyrolysis products.

INTRODUCTION

As a waste material in the bioethanol production and the celluloses industry lignin is a source for aromatic hydrocarbons. It is built up from three-dimensionally connected phenylpropane units, which upon thermal degradation are a rich source for phenolic compounds for synthesis of chemicals (1) to (3).

One of the most promising concepts for the thermal decomposition of lignin is to use a circulating fluidised bed (CFB) reactor for pyrolysis. The benefits of the use of a CFB system are the short residence time of the pyrolysis vapours (the desired product) and a high heating rate of the lignin, which are necessary to prevent further degradation reactions and to achieve a high yield of liquid product. By-products of the endothermic pyrolysis are non-condensable gases and char (4).

The aim of the present project is to optimize the endothermic pyrolysis process energetically by integrating the combustion of the by-products into the solids circulation loop of the CFB, by means of a bubbling fluidized bed. Furthermore, as char components have been reported to catalyze secondary reactions of the products to form lighter compounds (1, 5 and 6), the effect of catalysis shall be minimized by the integrated combustion of the char.

EXPERIMENTAL

To determine the design parameters for an integrated pyrolysis-combustion system, experiments in a CFB pyrolysis reactor (Figure 1) with riser diameter of 80 mm and a height of 1700 mm have been carried out at different operating conditions (Table 1). The lignin was pneumatically fed into the reactor through a nozzle with 6 mm diameter at a velocity of 40 m/s. The superficial velocity directly above the distributor

plate $u_{0,b}$ is given in Table 1 as well as $u_{0,t}$ which is the superficial velocity at the riser top, which includes the lignin conveying N_2 as well as the pyrolysis gas and the steam from vaporization of the lignin humidity. The solids flux in the riser could not be measured. The composition of the non-condensable, permanent gas has been monitored continuously throughout the experiments. The bed material (BM) as well as the material from the secondary cyclone (2C) have been collected after each test. The material properties, i.e. composition, particle morphology, particle size distribution and particle density were analyzed.

These properties have been used to determine the char combustion kinetics in a laboratory-size fluidized bed reactor. At the temperatures 700, 750, 800, 850 and 900 °C the samples of the materials with known mass m_S and carbon content γ_C were injected batchwise into the reactor. The gas composition of the flue gas was monitored and used to calculate the conversion $X_{char}(t)$.

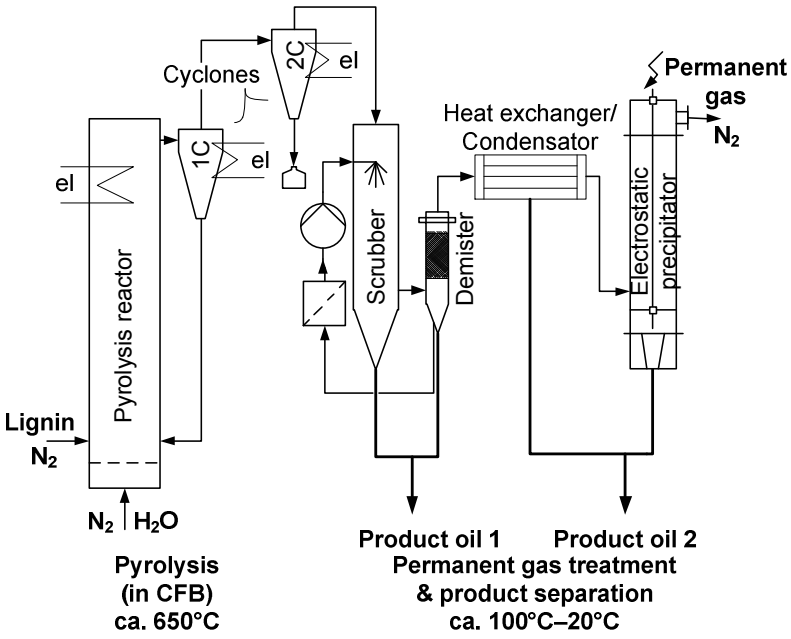

Figure 1: Experimental pyrolysis plant (80 mm riser diameter)

Moreover, the gross calorific values of the gas and the char together with their yields were compared with the required heat for pyrolysis. The latter was estimated by a simultaneous differential scanning calorimetry – thermogravimetric analysis (DSC-TGA) experiment of lignin. In the experiment two lignin samples were heated in an argon environment at a heating rate of 10 K/min in a thermal analysis apparatus, type NETZSCH STA F1 Jupiter between room temperature and 900 °C. The gross calorific value of the char was determined by experiments with an adiabatic calorimeter.

Table 1: Pyrolysis conditions

Exp.	Lignin		Fluidisation by steam		Gas velocity at	Pyrolysis
No.	Feed rate	u_{N2}	H_2O	$u_{0,b}$	riser top $u_{0,t}$	temperature
	kg/h	m/s	kg/h	m/s	m/s	°C
1	2.76	40	24	5	5.7	650
2	2.57	40	24	5	5.7	600

THEORY

Due to the nature of the bed material particles, i.e. the char layer on the quartz sand, the shrinking particle model (7) is modified, so that the particle shrinks upon

combustion until the inert sand core is reached. The modified model is subsequently derived and called shrinking particle inert-core model.

Shrinking Particle Inert Core-Model

The shrinking of a particle can be described as follows:

$$-\rho_{\text{char}} \frac{\mathrm{d}R}{\mathrm{d}t} = kC_{\mathrm{O}_2}^{n} \tag{1}$$

Therein ρ_{char} is the density of the char, R_{P} the mean radius of the char laden particle at the entrance of the fluidized bed combustor, k the reaction rate constant, C_{O_2} the mean oxygen concentration in the whole bed during the reaction, t the time and n the reaction order. With the burnout time $t = \tau$ and the radius of the quartz sand core $R = R_{\text{QS}}$, the integration gives

$$\tau = \frac{\rho_{\text{char}} \cdot (R_{\text{P}} - R_{\text{QS}})}{kC_{\mathrm{O}_2}^{n}} \tag{2}$$

Analogously for an arbitrary time $t < \tau$:

$$t = \frac{\rho_{\text{char}} \cdot (R_{\text{P}} - R)}{kC_{\mathrm{O}_2}^{n}} \tag{3}$$

Dividing Eq. (3) by Eq. (2) results in

$$\frac{t}{\tau} = K_1 \cdot \left(1 - \frac{R}{R_{\text{P}}}\right) \tag{4}$$

with $K_1 = 1/\left(1 - R_{\text{QS}} / R_{\text{P}}\right)$. For a particle with inert core the conversion X_{char} can be expressed as

$$1 - X_{\text{char}} = \frac{\text{volume unreacted char}}{\text{total char volume}} = \frac{\frac{4}{3}\pi\left(R^3 - R_{\text{QS}}^3\right)}{\frac{4}{3}\pi\left(R_{\text{P}}^3 - R_{\text{QS}}^3\right)} = K_2 \cdot \left(R^3 - R_{\text{QS}}^3\right) \tag{5}$$

with $K_2 = 1/\left(R_{\text{P}}^3 - R_{\text{QS}}^3\right)$. Solving Eq. (5) for R and replacing R by the result in Eq. (4) with subsequent differentiation results in

$$\begin{aligned} \frac{\mathrm{d}X_{\text{char}}}{\mathrm{d}t} &= \frac{3\mathrm{R}_{\text{P}}^3 K_2}{\tau \mathrm{K}_1} \cdot \left(\frac{1 - X_{\text{char}}}{\mathrm{R}_{\text{P}}^3 K_2} + \left(\frac{R_{\text{QS}}}{R_{\text{P}}} \right)^3 \right)^{\frac{2}{3}} \\ &= \frac{3\mathrm{R}_{\text{P}}^2 K_2 \cdot kC_{\mathrm{O}_2}^{n}}{\rho_{\text{char}}} \cdot \left(\frac{1 - X_{\text{char}}}{\mathrm{R}_{\text{P}}^3 K_2} + \left(\frac{R_{\text{QS}}}{R_{\text{P}}} \right)^3 \right)^{\frac{2}{3}} \end{aligned} \tag{6}$$

It should be noted that with $R_{\text{QS}} = 0$ the equation reduces to the shrinking particle formulation, that can be found in (7). The radius of the inert quartz sand core R_{QS} is calculated by the difference $R_{\text{QS}} = R_{\text{P}} - d$.

RESULTS

Pyrolysis Conditions and Solids Properties

For the determination of combustion kinetics it is necessary, that the composition of the solid fuel (proximate and ultimate analysis), its density and morphology as well as particle size distribution are known. The proximate as well as ultimate analysis for the bed material (BM) and the material collected by the secondary cyclone (2C) are listed, in Table 2. The difference of the inert and the ash fraction is equal to the sand

Table 2: Proximate and ultimate analysis as well as gross calorific value of solid materials used for experiments

Sample	Sample composition (wt.-%)										HHV
	Proximate analysis					Ultimate analysis					
	Water	Vola-tiles	C_{Fix}	Inert	Ash	C	H	N	S	O	MJ/kg
Lignin	5.3	66.0	27.5	1.2	1.2	58.8	5.3	0.4	1.7	27.3	25.2
BM Exp. 1	0.7	1.5	6.9	90.9	12.1	9.3	0.3	0.0	0.3	0.0	29.0
2C Exp. 1	1.1	1.9	11.1	85.9	12.1	16.8	0.4	0.0	0.3	0.0	29.7
BM Exp. 2	0.8	1.4	7.3	90.5	7.2	8.2	0.3	0.0	0.2	0.0	30.2
2C Exp. 2	1.0	2.1	9.9	87.0	7.2	10.6	0.3	0.0	0.3	0.8	28.6

Reference state: raw except HHV: inert free; Water content of lignin at 60 °C (due to reactions at temperatures above 66 °C)

fraction in the sample. The ash contents of the bed material as well as the secondary cyclone material have been calculated by the ash content of the lignin divided by the char yield Y_C. Latter is calculated by dividing the integral char mass after an experiment by the integral of the fed raw lignin mass during the experiment:

$$Y_C = \frac{m_{\text{bed material after exp.}} + m_{\text{2C material after exp.}} - m_{\text{bed material before exp.}}}{m_{\text{lignin fed during exp.}}} \quad (7)$$

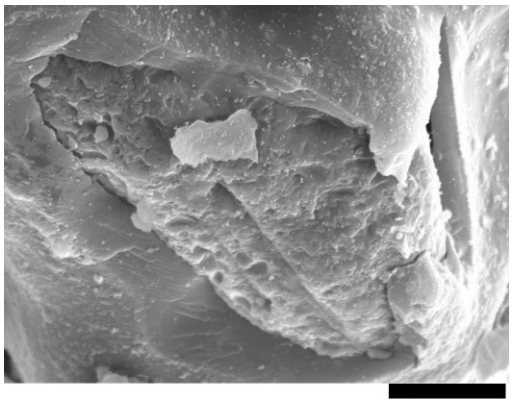

Figure 2: SEM of the surface structure of a bed material particle's coating fracture, scale bar is 10 µm

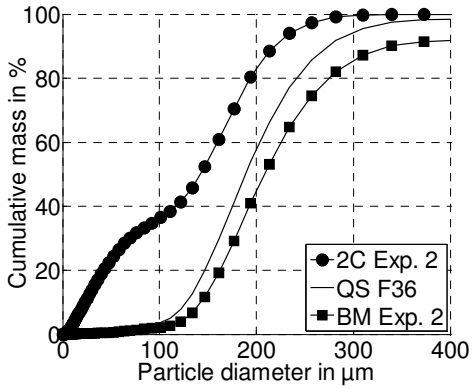

Figure 3: Exemplarily particle size distribution of BM and 2C of Exp 2 in comparison with quartz sand

A SEM image of the bed material after pyrolysis experiment is shown in Figure 2. On the picture a sand particle coated with a char layer can be recognized, with part of the char layer broken apart. The particle size distribution of the secondary cyclone

material (2C) is bimodal, while the distributions of the quartz sand and the bed material (BM) are monomodal (Figure 3). This is due to the fragments of the char coating shells, which are mainly found in the secondary cyclone material. The char density ρ_{char} was calculated from the composition of the bed material and the densities of bed material and quartz sand. The average char layer thickness *d* has been calculated, using the assumption of spherical particles.

Table 3: Sauter mean diameter D_S, char layer thickness d and densities ρ_{QS} of the quartz sand and ρ_P of the bed material and the corresponding ρ_{char} of the char

Sample	D_S µm	d µm	ρ_{QS}/ ρ_P g/cm^3	ρ_{char} g/cm^3
Quartz sand	39.2	--	2.63	--
BM Exp. 1	78.8	9.0	2.50	0.81
2C Exp. 1	35.8	--	--	--
BM Exp. 2	129.5	15.5	2.50	1.03
2C Exp. 2	45.0	--	--	--

These calculations have been validated by dimensioning of char layer fragments in several SEM images (0.6 to 18.1 µm). The results are listed in Table 3.

Combustion Kinetics

The conversion of the char X_{char} at an arbitrary time *t* is defined as the conversion of carbon at that time. Therefore, the measured carbon content in the flue gas, integrated over the time, is divided by the initial carbon mass of the sample:

$$X_{\text{char}} = \frac{m_{\text{C}}(t) \text{ in } \text{CO}_2}{m_{\text{S}} \cdot \gamma_{\text{C}}} \tag{8}$$

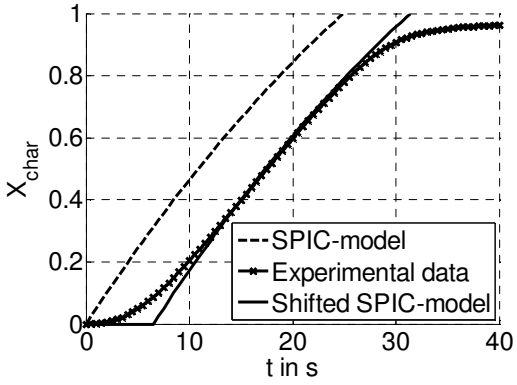

Figure 4: Conversion of a BM Exp. 1 sample in a combustion experiment at 850°C and the correlative Shrinking Particle Inert Core kinetic model conversion

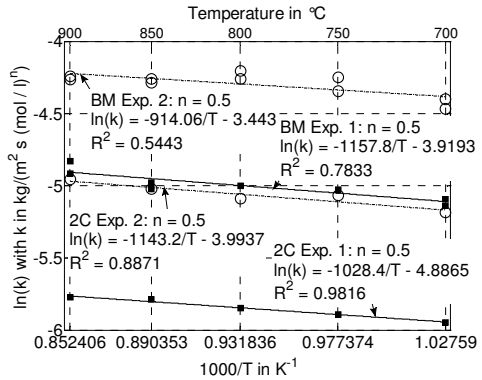

Figure 5: Arrhenius-plot of the analysed materials

The measured values X_{char}(t) were fitted by the Shrinking Particle Inert Core-model (Eq. (6)) with the fitting parameters *k* and *n*. An example of both curves for BM Exp. 1 is given in Figure 4. Other than predicted by the Shrinking Particle Inert Core-model, the slope of the conversion-curve is not maximal at the beginning and also much smaller at higher reaction times than expected. Because of the experimental setup, which comprises a quite long duct between the reactor and the online gas measurement as well as a gas filter, dispersion effects cause the deviation. This was checked by the introduction of a known square pulse to the reactor. The pulse response needed about 8 s to reach the pulse amplitude and the decay took about 16 s. These durations approximately relate to the response and

decay times in Figure 4. Therefore, the conversion curve computed by the Shrinking Particle Inert Core-model was shifted by 8 s (Figure 4).

The resulting Arrhenius-plots for the four tested materials are shown in Figure 5 in the temperature interval of 700 to 900°C with the obtained values for *n* and *k*.

Energy Balance

To establish an energy balance for the pyrolysis system with integrated by-product combustion, the total heat release of the by-products related to the fed raw lignin mass and the mass specific heat demand for lignin pyrolysis are specified below. The combustion of the by-products shall take place at 850°C. Heat losses and auxiliary energy demand, e.g. for feeding of lignin and preheating of the fluidisation gas, have not been considered.

Pyrolysis Energy Requirement

The results of the thermal analysis of lignin are shown in Figure 6. It is very probable that the first mass loss step belongs to the loss of moisture, whereas the other steps are caused by devolatilization and pyrolytic cracking of the sample.

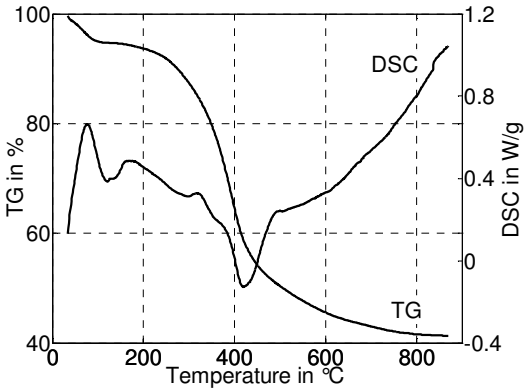

Figure 6: Thermal analysis of lignin (DSC and TGA)

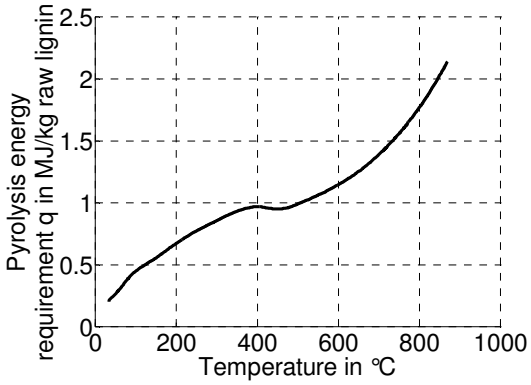

Figure 7: Approx. pyrolysis energy requirement per kg raw lignin

According to the mass loss endothermic or exothermic effects can be seen in the DSC curve. The enthalpy of the single effects is difficult to determine, because the effects interfere with each other. In the temperature interval of 200°C to 350°C it can not be differentiated between endothermic or exothermic behaviour. To calculate the energy demand for the pyrolysis the integral of the DSC signal $\dot{q}$ is used (Eq. (9)).

$$q = \frac{1}{\beta} \cdot \int_{T_0}^{T} \dot{q} \, \mathrm{d}T = \int_{t_0}^{t} \dot{q} \, \mathrm{d}t \tag{9}$$

The results are shown in Figure 7. The specific heat is related to the initial mass of raw lignin. For the pyrolysis at a temperature of 650°C a mean value of about 1300 kJ/kg of raw lignin for the energy demand can be calculated.

Energy Supply

The yield of permanent gases, which contribute to a heat release upon combustion (CO, CO_2, H_2, C_1-C_4 as CH_4) rises with rising temperature. This result coincides with the observations of Wei et al. (8), Scott and Piskorz (9), Zheng (10) and Di Blasi (11). As with rising temperature secondary cracking reactions are favoured, the more complex char and liquid molecules are converted to gases. Our measurements have shown, that the composition of the permanent gas mixture does not change considerably. This trend can also be found for the total heat release by the combustion of permanent gas per mass of raw lignin fed to the pyrolysis. The results are shown in Figure 8.

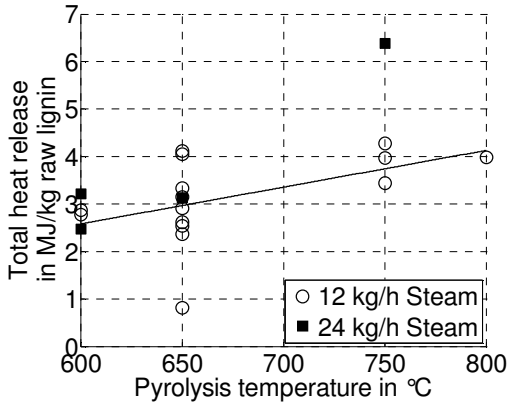

Figure 8: Total heat release of permanent gas combustion per kg raw lignin (combustion at 850°C)

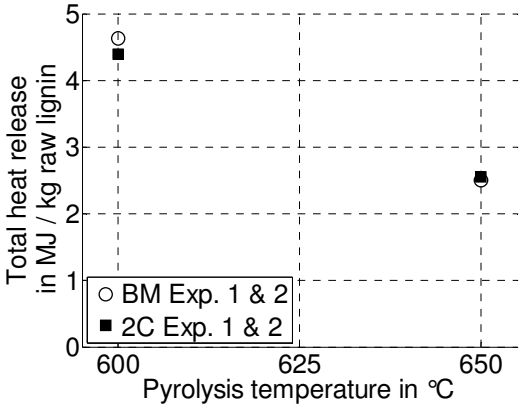

Figure 9: Total heat release of char combustion per kg raw lignin (combustion at 850°C)

On the other hand, because of secondary reactions as explained above, the yield of char decreases with rising temperature, while the gross calorific value does not change significantly (see Table 2). Therefore, the lignin specific total heat release of char combustion decreases with rising temperature. This can be seen in Figure 9 and is in good agreement with the above cited literature.

At a pyrolysis temperature of 650°C, the energy demand for lignin pyrolysis is about 1500 kJ/kg_L. The combustion of the by-products at this temperature releases about 3000 kJ/kg_L for the permanent gases and 2500 kJ/kg_L for the char. In the integrated pyrolysis-combustion process this gives an energy surplus of 4000 kJ/kg_L.

SUMMARY AND CONCLUSIONS

To couple a pyrolysis CFB reactor with an integrated combustion of the pyrolysis by-products, char properties, combustion kinetics and the energy balance have been investigated.

The quartz sand particles, which make up the bed material, are coated with char. Therefore, a model for combustion kinetics has been derived, which accounts for the fact that only a char layer with certain thickness is combusted. For the investigated materials, the combustion kinetics have been determined by combustion experiments in a laboratory scale fluidized bed. The combustion kinetics model does fit the experimental data well.

The energy demand for lignin pyrolysis has been estimated by differential scanning calorimetry. Pyrolysis experiments in a CFB reactor (80 mm diameter) were carried out to identify the lignin specific energy in the by-products. At the pyrolysis temperature of 650°C the combustion of permanent gases and char generates an energy surplus of 4000 kJ/kg_L. The surplus can be used for preheating the fluidization gases and balancing the heat losses.
The obtained data is currently used to design a circulating fluidized bed pyrolysis reactor with integrated fluidized bed combustor.

ACKNOWLEDGEMENT

This work has been carried out within the framework of the cluster Biorefinery2021, funded by the German Federal Ministry of Research and Technology (FKZ 0315559A). The responsibility for the content of this work lies with the authors.

NOTATION

C	Concentration	
d	Char layer thickness	µm
D_S	Sauter mean diameter	µm
k	Reaction rate constant	$kg/(m^2s(mol/l)^n)$
K	Constant	--
m	Mass	kg
n	Reaction order	--
q	Mass specific energy	kJ/kg
$\dot{q}$	Mass specific heat flux	W/kg
R	Radius	µm
t	time	s
T	Temperature	K
X	Conversion	--
Y	Yield	--
β	Heating rate	K/min
γ	Mass fraction	--
υ	Temperature	°C
ρ	Density	kg/m^3
τ	Burnout time	s

Subscripts

char	Char
C	Carbon
L	raw Lignin
P	Particle
QS	Quartz sand
S	Sample, Sauter

REFERENCES

(1) Amen-Chen C., Pakdel H., Roy C. (2001), Bioresource Technology 79, 3, 277–299.
(2) Bridgwater A. V., Meier D., Radlein D. (1999), Organic Geochemistry 30, 12, 1479–1493.
(3) Bridgwater A. V. (2003), Chemical Engineering Journal 91, 2-3, 87–102.
(4) Basu P. (2010) Biomass gasification and pyrolysis, Elsevier/AP. Amsterdam
(5) Park H., Park Y., Dong J., Jeon J., Kim S., Kim J. et al. (2009), Fuel Processing Technology 90, 2, 186–195.
(6) Asadullah M., Anisur Rahman M., Mohsin Ali M., Abdul Motin M., Borhanus Sultan M., Robiul Alam M., Sahedur Rahman M. (2008), Bioresource Technology 99, 1, 44–50.
(7) Levenspiel O. (1999) Chemical reaction engineering, Wiley. Hoboken, NJ.
(8) Wei L. G., Xu S. P., Zhang L., Zhang H. G., Liu C. H., Zhu H., Liu S. Q. (2006), Fuel Processing Technology 87, 10, 863–871.
(9) Scott D. S., Piskorz J. (1982), Canadian Journal of Chemical Engineering 60, 5, 666–674.
(10) Zheng J. L. (2007), Journal of Analytical and Applied Pyrolysis 80, 1, 30–35.
(11) Di Blasi C. (2009), Progress in energy and combustion science 35, 2, 121–140.